

Fig. 2. Schematic of the preamplifier, master latch, slave latch, and output buffer.

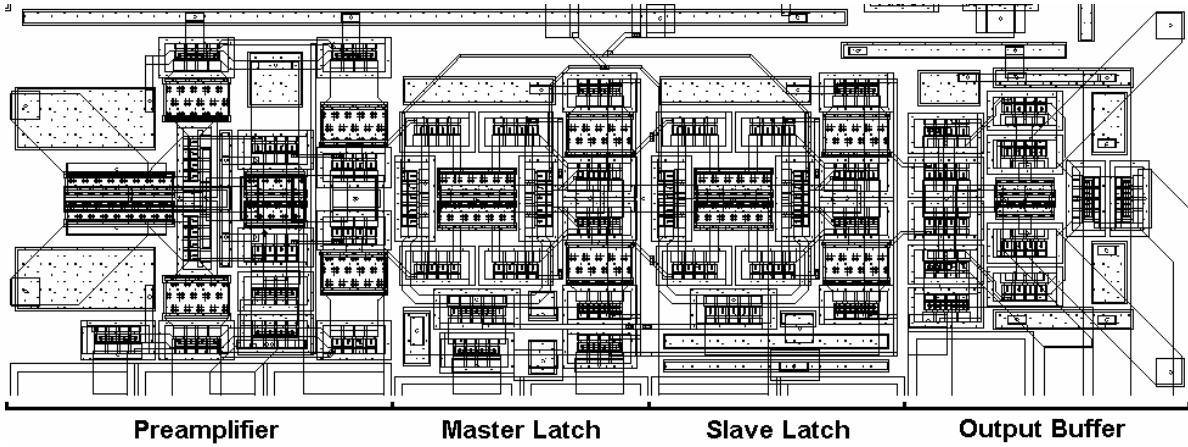


Fig. 3. Symmetrical and compact layout of the preamplifier, master latch, slave latch, and output buffer, occupying  $210 \times 62 \mu\text{m}^2$ .

pairs current switched by a series-gated clock in an ECL configuration. The maximum sampling rate of the latch is determined by the recovery time

$$t_{rec} = R_L C_{total} \left( 1 + \frac{1}{\tanh(V_{in}/2V_T)} \right), \quad (1)$$

where  $R_L$  is the load resistance,  $C_{total}$  is the total capacitance at collector of first differential pair ( $Q_7$ - $Q_8$  and  $Q_{15}$ - $Q_{16}$ ),  $V_{in}$  is the differential input voltage of the latch, and  $V_T$  is the thermal voltage, as well as the regeneration time constant

$$\tau_{reg} = \frac{R_L C_{total}}{g_m R_L - 1}, \quad (2)$$

where  $g_m$  is the transconductance of the HBTs in the second differential pair ( $Q_{10}$ - $Q_{11}$  and  $Q_{18}$ - $Q_{19}$ ), with the  $t_{rec}$  being the dominating factor [4]. Thus to shorten  $t_{rec}$ , a small  $R_L$  is desired. However, a small  $R_L$  will also reduce the output voltage swing of the latch and in turn degrade the current switch operation of the second differential pair [5]. Based on simulations, a compromise was made with  $R_L$  of  $90 \Omega$ , resulting in a  $t_{rec}$  of 19

ps for a  $V_{in}$  of 7 mV. The output buffer, also on-chip  $50 \Omega$  terminated, is introduced to drive the test equipment without loading the output of the slave latch.

Proper layout is critical as circuit performance increases to the tens of GHz frequency range. High-speed operation can be strongly degraded by the parasitics introduced during layout, and special care must be taken to control their impact. To minimize common-mode noise, the layout is made as symmetrical as possible. Crossing area between metal routing are kept small to reduce crossing capacitance without increasing series resistance or violating electromigration rules. Interconnects in the critical path are kept short to curve layout parasitics. Auto-filler blocking layer are added to prevent unintentionally altering the microwave behavior of the propagating signals. Tapered lines are used, and  $90^\circ$  turns are avoided to minimize internal reflections. Fig. 3 shows the symmetrical and compact layout of the preamplifier, M/S latches, and output buffer. On-chip by-pass MIM capacitors are used on  $dc$  supply lines for high-frequency decoupling. Connections from the preamplifier, clock buffer, and output buffer to the bondpads are distributed towards the left, top, and right side, respectively, to facilitate on-wafer testing. Twelve

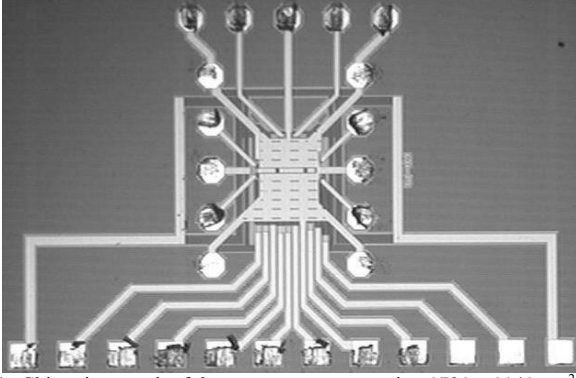


Fig. 4. Chip micrograph of the comparator, occupying  $1731 \times 1141 \mu\text{m}^2$ .

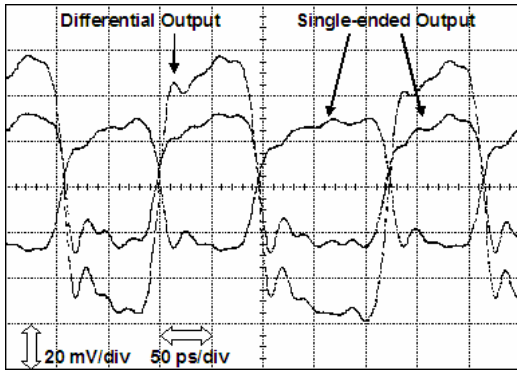


Fig. 5. Measured output waveforms of the comparator with a 5 GHz input oversampled at 32 GS/s (20 mV/div, 50 ps/div).

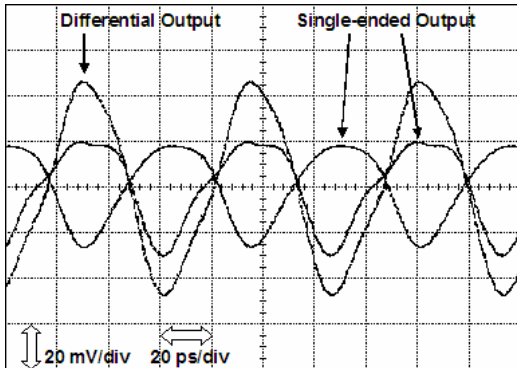


Fig. 6. Measured output waveforms of the comparator operating at Nyquist with a sampling rate of 30 GS/s (20 mV/div, 20 ps/div).

*dc* supply lines, used for current monitoring, are dispersed to the bottom side.

#### IV. MEASUREMENT RESULTS

The chip micrograph of the comparator is shown in Fig. 4. The total die area is  $1731 \times 1141 \mu\text{m}^2$  (including bondpads). The large width of the chip is determined by the footprint of the 12 pin *dc* probes (for current monitoring). The active area of the preamplifier, M/S latches, and output buffer is  $210 \times 62 \mu\text{m}^2$ , and  $82 \times 116 \mu\text{m}^2$  for the clock buffer.

The comparator is characterized on-wafer using 40 GHz

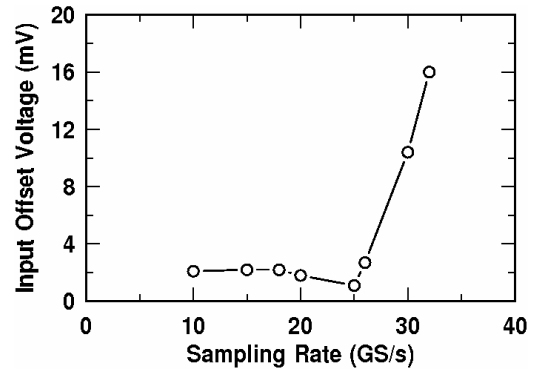


Fig. 7. Measured input offset voltage of the comparator as a function of sampling rate.

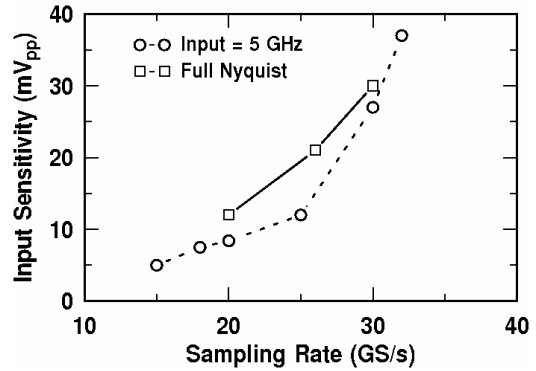


Fig. 8. Measured input sensitivity of the comparator as a function of sampling rate.

probes and cables. Hybrids and baluns are used to convert single-ended signals into differential ones. Phase tuners are used to compensate for different cable phase characteristics before connecting them into the test setup to ensure that the phase of complementary signals are properly maintained since any asymmetry caused by external testing equipments will degrade the performance of the comparator at high frequencies. Operating off a 3.5 V power supply, the comparator dissipates a total power of 405 mW, with the M/S latch core consuming 136 mW.

The comparator was tested with sine wave input and clock under two different conditions: (1) a 5 GHz input oversampled up to 32 GS/s; and (2) full Nyquist with sampling rates up to 30 GS/s. The output waveforms (both differential and single-ended) of the comparator operating with a 5 GHz input oversampled at 32 GS/s, shown in Fig. 5, measured a rise/fall time (20% to 80%) of 12.3/11.2 ps and a random (RMS)/deterministic (peak-to-peak) jitter of 1.15/5.59 ps. The output waveforms of the comparator operating at Nyquist with a sampling rate of 30 GS/s, shown in Fig. 6, measured a rise/fall time of 13.0/9.5 ps and a random/deterministic jitter of 1.09/5.80 ps.

The measured input offset voltage of the comparator, caused by device mismatch, as a function of sampling rate with *dc* input is shown in Fig. 7. The offset remains relatively constant at 2.2 mV when sampled below 18 GS/s, reaches a

TABLE II  
COMPARISON WITH PUBLISHED STAND-ALONE COMPARATORS OPERATING AT SIMILAR SAMPLING RATE

Reference	Maximum Sampling Rate [GS/s]	Sensitivity @ Input / Clock [@ GHz / GS/s]	Input Offset [mV]	Supply Voltage [V]	Total Power Consumption [mW]	Process / $f_T$ [- / GHz]	Active Area [mm <sup>2</sup> ]
This work	32	8.4 mV <sub>pp</sub> @ 5 / 20	< 2.2 up to 25 GS/s	3.5	405	SiGe / 200	0.0226
[6]	25	N/A	1.5 typical / 6 max	3.3	550	InP / N/A	N/A
[7]	20	8.9 mV <sub>pp</sub> @ 3 / 18	4.2 max	3.5	82 <sup>a</sup>	SiGe / 120	0.0455
[8]	16	N/A	N/A	N/A	221	SiGe / 55	0.0960
[9]	8	30 mV @ 4 / 8	N/A	-6	N/A	GaAs / 30	N/A

<sup>a</sup> Preamplifier and M/S latches only.

TABLE I  
PERFORMANCE SUMMARY OF THE COMPARATOR

Supply Voltage	3.5 V
Power Consumption	405 mW
Preamplifier	133 mW
Clock Buffer	90 mW
M/S Latches	136 mW
Output Buffer	46 mW
Input Range	1.2 V <sub>pp</sub> max
Sampling Rate	32 GS/s max
Rise/Fall Time (20% to 80%)	12.3 / 11.2 ps (in/clock = 5 GHz / 32 GS/s)
Random/Deterministic Jitter	1.09 / 5.80 ps (Nyquist, clock = 30 GS/s)
Input Offset Voltage	< 2.2 mV up to 25 GS/s
Input Sensitivity	8.4 mV <sub>pp</sub> (in/clock = 5 GHz / 20 GS/s)

minimum of 1.1 mV at 25 GS/s, and then increases to 16.7 mV at 32 GS/s.

Fig. 8 shows the input sensitivity of the comparator, defined as the minimum differential peak-to-peak input voltage that can be detected, as a function of sampling rate operating with a 5 GHz input and at Nyquist. With the 5 GHz input, the measured sensitivity ranges from 5 mV<sub>pp</sub> at 15 GS/s to 37 mV<sub>pp</sub> at 32 GS/s, equivalent to 7.9 bits and 5.0 bits of ADC resolution, respectively, for the full input range of 1.2 V<sub>pp</sub>. At Nyquist, the sensitivity ranges from 12 mV<sub>pp</sub> at 20 GS/s to 30 mV<sub>pp</sub> at 30 GS/s, equivalent to 6.6 bits and 5.3 bits of ADC resolution, respectively. This demonstrates that the comparator is well-suited for ultra-high-speed medium-resolution oversampled or Nyquist ADCs. The performance of the comparator is summarized in Table I.

Numerous comparators, either stand-alone or integrated into full ADCs, have been published in literature. Comparisons of this work to other high-speed stand-alone comparators are shown in Table II. Integrated comparators are omitted due to lack of direct measurement results on the comparators themselves. To our knowledge, this comparator achieves the best input sensitivity-sampling rate combination, offering significant benefit to the design of ultra-high-speed oversampled or Nyquist ADCs.

## V. SUMMARY

An ultra-high-speed comparator has been designed and fabricated in a 200 GHz SiGe HBT technology. The comparator can oversample a 5 GHz input up to 32 GS/s or sample at Nyquist up to 30 GS/s, while attaining 5.0 to 7.9 bits of ADC resolution. To our knowledge, this comparator achieves the best input sensitivity-sampling rate combination when compared with other published stand-alone comparators.

## ACKNOWLEDGMENT

This work was supported by the Georgia Electronic Design Center at Georgia Tech and IHP. The authors are grateful to C. Scholz of Georgia Tech and the IHP SiGe technology team for their contributions.

## REFERENCES

- [1] M. Hotta, K. Maio, N. Yokozawa, T. Watanabe, and S. Ueda, "A 150-mW 8-bit video-frequency A/D converter," *IEEE J. Solid-State Circuits*, vol. 21, pp. 318-323, Apr. 1986.
- [2] B. Heinemann, H. Rücker, R. Barth, J. Bauer, D. Bolze, E. Bugiel, J. Drews, K.-E. Ehwald, T. Grabolla, U. Haak, W. Höppner, D. Knoll, D. Krüger, B. Kuck, R. Kurps, M. Marschmeyer, H.H. Richter, P. Schley, D. Schmidt, R. Scholz, B. Tillack, W. Winkler, D. Wolansky, H.-E. Wulf, Y. Yamamoto, and P. Zaumseil, "Novel collector design for high-speed SiGe:C HBTs," in *IEEE Technical Dig. of IEDM*, Dec. 2002, pp. 775-778.
- [3] B. Razavi, *Principles of Data Conversion System Design*. Piscataway, NJ: IEEE Press, 1995.
- [4] P. J. Lim and B. A. Wooley, "An 8-bit 200-MHz BiCMOS comparator," *IEEE J. Solid-State Circuits*, vol. 25, pp. 192-199, Feb. 1990.
- [5] W. Gao, W. M. Snelgrove, and S. J. Kovacic, "A 5-GHz SiGe HBT return-to-zero comparator for RF A/D conversion," *IEEE J. Solid-State Circuits*, vol. 31, pp. 1502-1506, Oct. 1996.
- [6] *25707CP 25 GHz Latched Comparator Data Sheet*, Inphi Corp., Westlake Village, CA.
- [7] X. Li, W.-M.L. Kuo, Y. Lu, R. Krithivasan, T. Chen, J.D. Cressler, and A.J. Joseph, "A 7-bit, 18 GHz SiGe HBT comparator for medium resolution A/D conversion," to appear in *Proc. IEEE BCTM*, 2005.
- [8] J.C. Jensen and L.E. Larson, "A 16-GHz ultra-high-speed Si-SiGe HBT comparator," *IEEE J. Solid-State Circuits*, vol. 38, pp. 1584-1589, Sept. 2003.
- [9] D. Selle, D. Carisetti, T. Ducourant, P. Bertsch, and P. Boissenot, "8GHz full Nyquist HBT comparator," *Electron. Lett.*, vol. 26, pp. 919-921, Jun. 1990.